Electronic Supplementary Material (ESI) for Catalysis Science & Technology.

Supporting Information

for

Nanobelt α-CuV_2O_6 with hydrophilic mesoporous poly(ionic liquid): Binary catalyst for one-pot and one-step conversion of fructose into 2,5-diformylfuran

Wei Hou, Qian Wang, Zengjing Guo, Jing Li, Yu Zhou, Jun Wang**

State Key Laboratory of Materials-Oriented Chemical Engineering, College of Chemical Engineering, Nanjing Tech University (formerly Nanjing University of Technology), Nanjing, 210009, China

* Corresponding author: njutzhouyu@njtech.edu.cn (Y. Zhou), junwang@njtech.edu.cn (J. Wang)

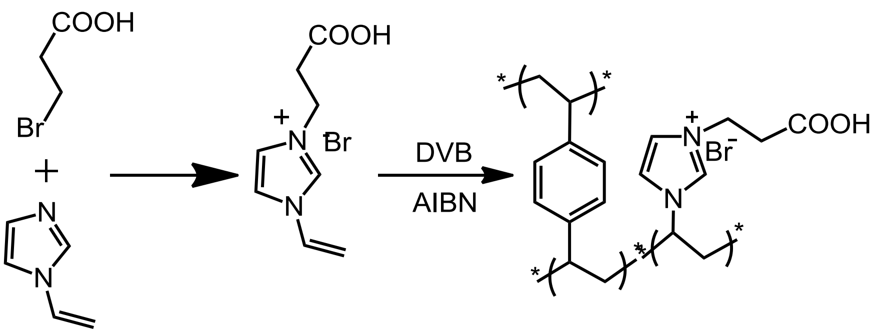

Scheme S1. Synthesis of P(DVPI-Br).

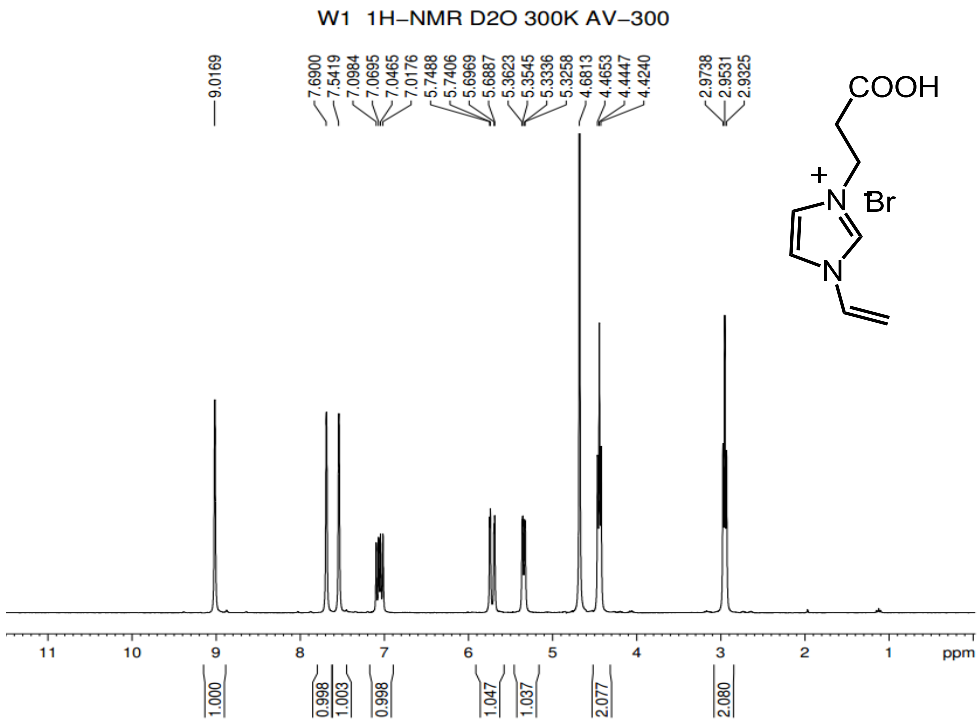

Fig. S1. ^{1}H-NMR spectrum of VPI-Br.

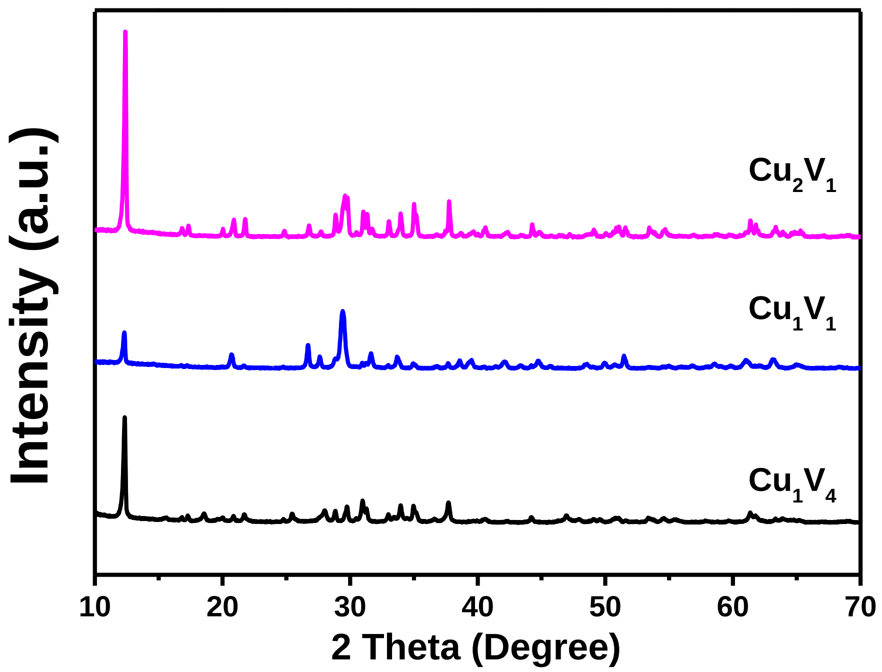

Fig. S2. XRD patterns of Cu_2V_1, Cu_1V_1 and Cu_1V_4.

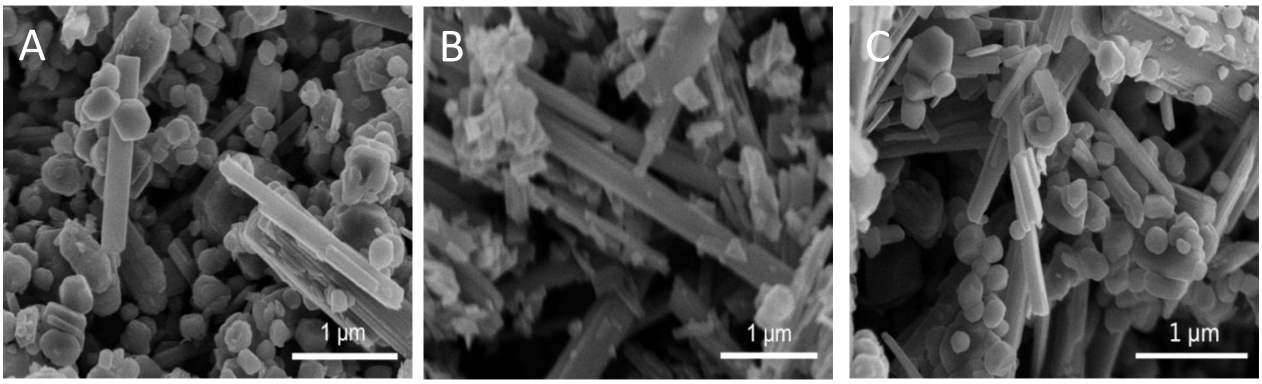

Fig. S3. SEM images of (A) Cu_2V_1 (B) Cu_1V_1 and (C) Cu_1V_4.

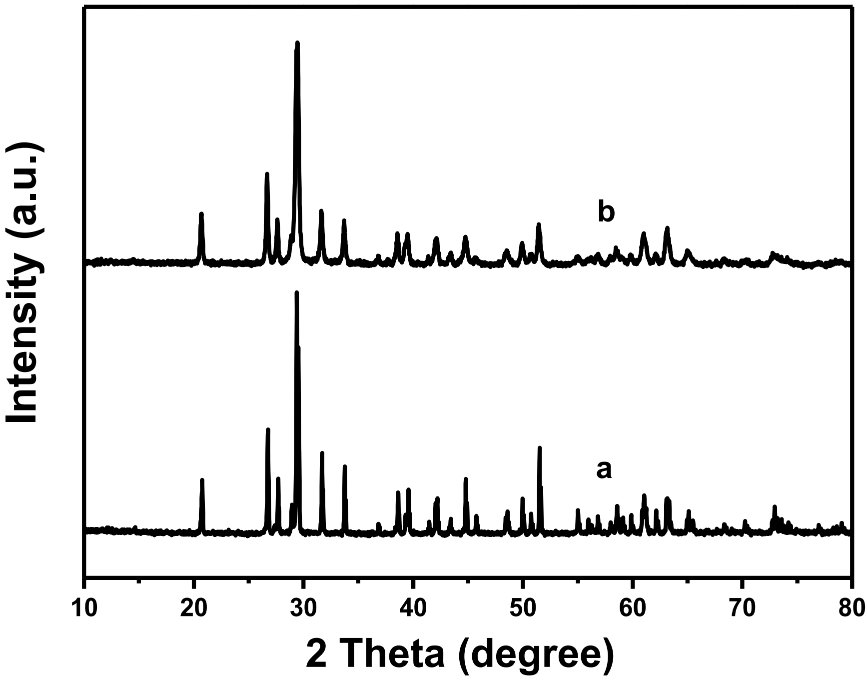

Fig. S4. XRD patterns of (a) α-CuV_2O_6 and (b) α-CuV_2O_6-B.

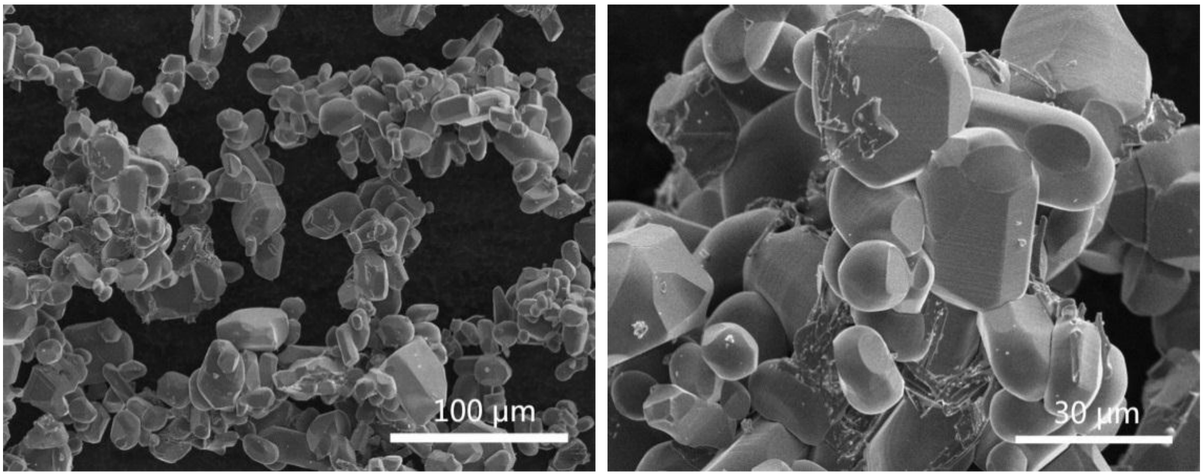

Fig. S5. SEM images of α-CuV_2O_6-B.

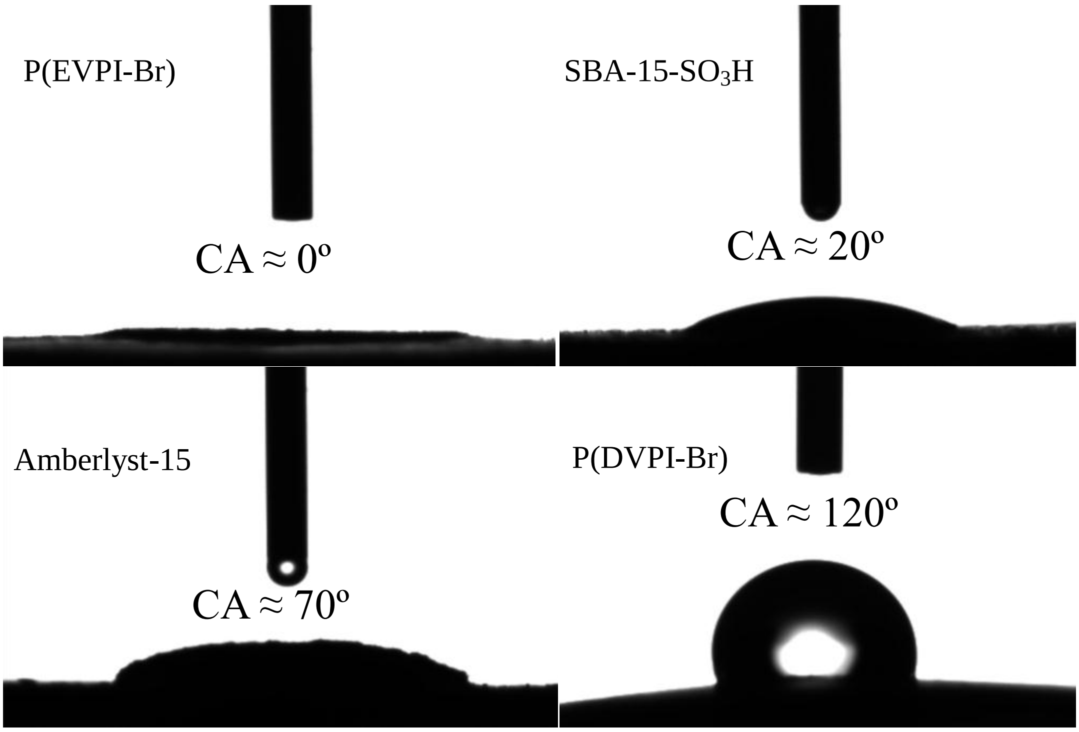

Fig. S6. Contact angles of water droplet on the surface of different acid catalysts.

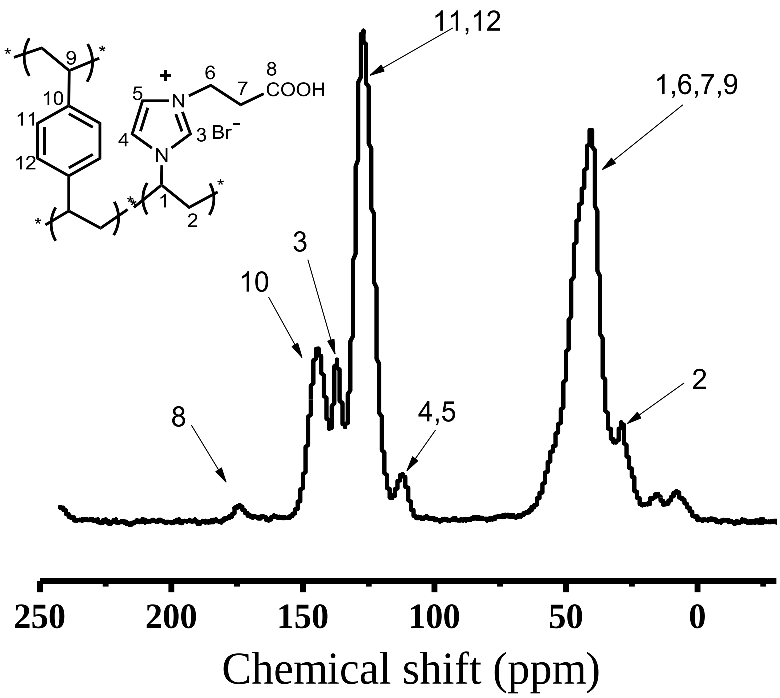

Fig. S7. ^{13}C MAS NMR spectrum of P(DVPI-Br).

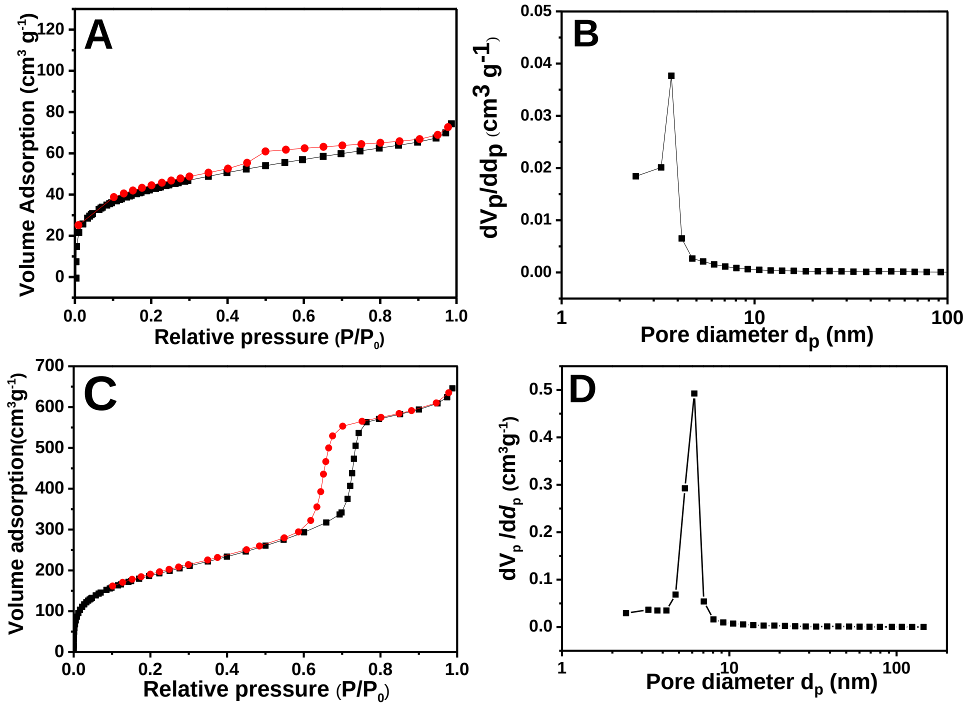

Figure S8. N_2 adsorption isotherms and pore size distribution curves of (A, B) P(DVPI-Br) and (C, D) SBA-15-SO_3H.

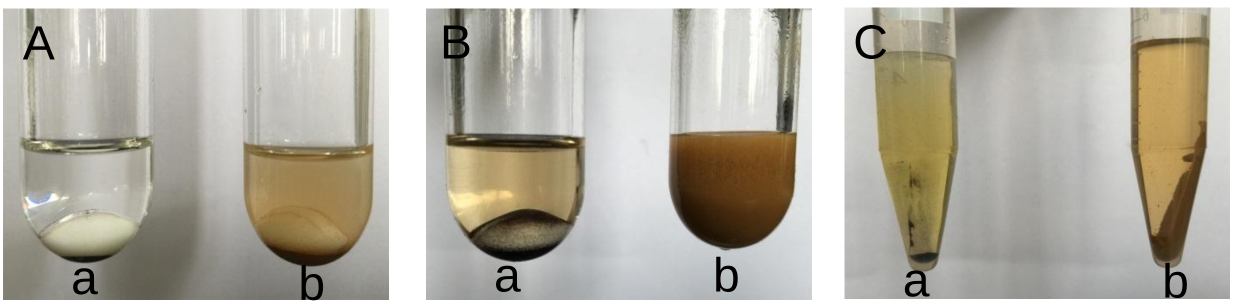

Fig. S9. Reaction solution (A) before reaction, (B) after reaction and (C) after centrifugation in the (a) α-CuV_2O_6-B and (b) α-CuV_2O_6 catalyzed conversion of HMF into DFF. Reaction conditions: HMF (1 mmol), α-CuV_2O_6 (0.04 g), solvent (DMSO, 4 mL), O_2 balloon (1 bar), 130 ℃, 3 h.

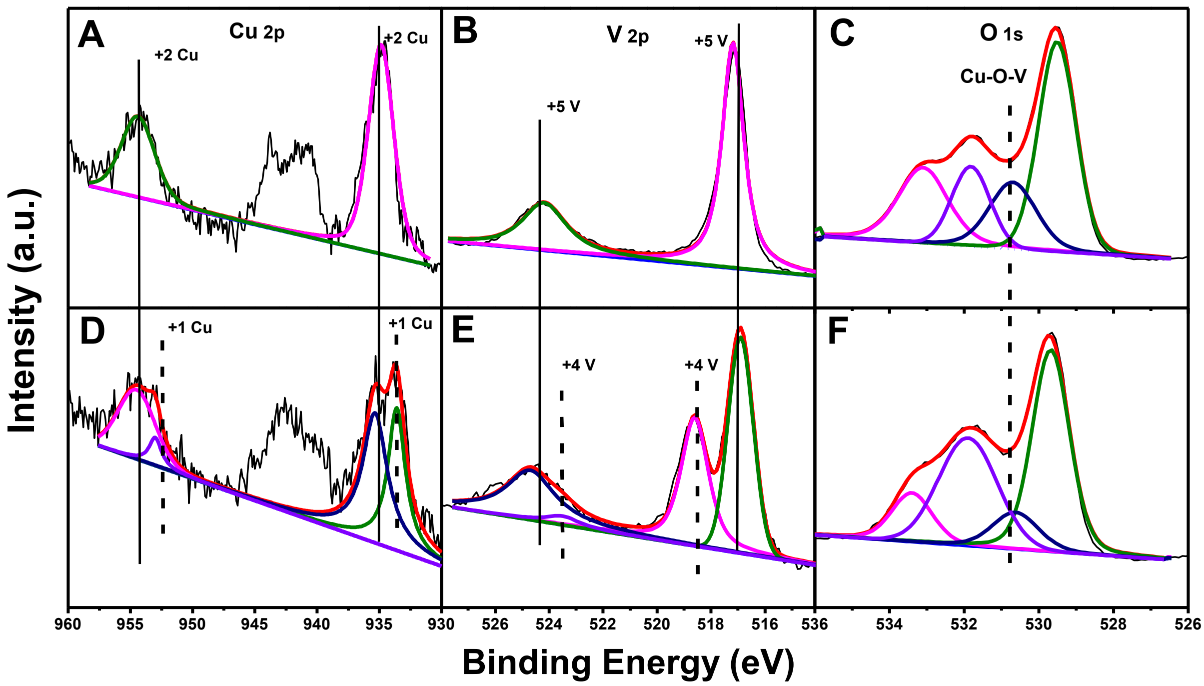

Fig. S10. XPS analyses of recovered α-CuV_2O_6 in the conversion of HMF into DFF under (A, B, C) O_2 and (D, E, F) N_2 condition.

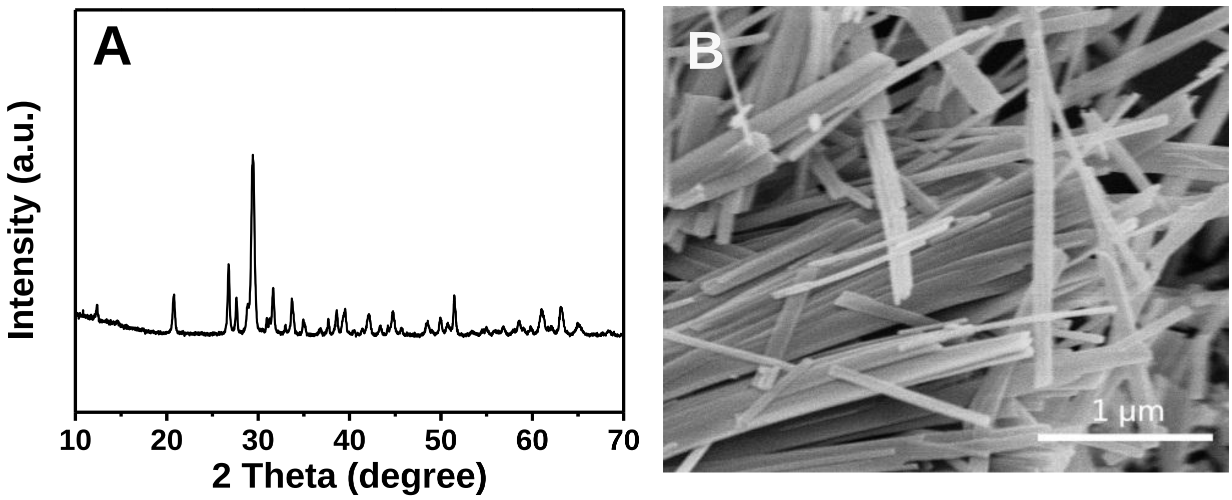

Fig. S11. (A) XRD patterns and (B) SEM image of recovered α-CuV_2O_6.

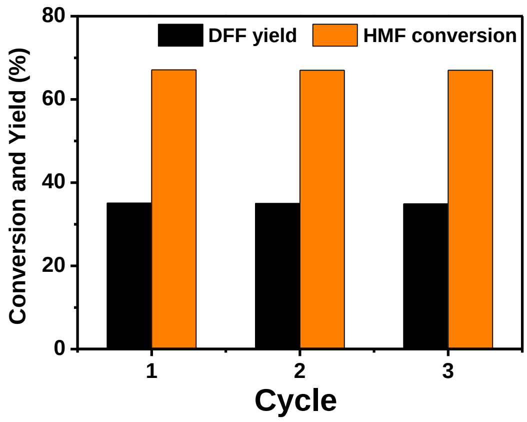

Fig. S12. Recyclability of α-CuV_2O_6 in the oxidation of HMF. Reaction conditions: HMF (1 mmol), α-CuV_2O_6 (0.04 g), solvent (DMSO, 4 mL), O_2 balloon (1 bar), 130 ℃, 1 h.

Table S1. Summary of the corresponding morphology and phase of the products.

Sample	Feeding ratio of Cu/V (mol/mol)	Morphology	Phase[a]	Detected Cu/V (mol/mol)[b]
Cu_2V_1	2:1	sphere and rod	CuV_2O (630-0513) and $Cu_3(OH)_2V_2O_7 \cdot 2H_2O$ (46-1443)	1.4
Cu_1V_1	1:1	particle and rod	CuV_2O_6 (630-0513) and $Cu_{2.33}V_4O_{11}$ (54-1241)	0.8
Cu_1V_2 (α-CuV_2O_6)	1:2	nanobelt	CuV_2O_6 (630-0513)	0.5
Cu_1V_4	1:4	particle and rod	CuV_2O_6 (630-0513) and $Cu_{0.4}V_2O_5$ (46-0361)	0.3

[a]Phases are determined by using the MDI Jade software (Jade 6 XRD Pattern processing Software) and the corresponding JCPDS card no. is shown in bracket. [b]Mole ratio of Cu to V is detected by inductively coupled plasma mass spectrometry (ICP).

Table S2. Elemental analysis of IL monomer and acid catalysts.

Entry	Sample	C (%)	H (%)	S (%)	N (%)
1	VPI-Br	38.81	4.36	-	11.24
2	P(EVPI-Br)	60.97	5.86	-	3.68
3	P(DVPI-Br)	65.09	6.06	-	3.65
4	Amberlyst-15	56.1	5.67	13.76	-
5	SBA-15-SO_3H	11.2	3.81	8.6	-

Table S3. The catalytic performances in the aerobic oxidation of HMF to DFF under atmospheric pressure over various heterogeneous catalysts.

Catalyst	T, t & P[a]	HMF/Catalyst (mg/mg)	C_{HMF}[b] (%)	S_{DFF}[c] (%)	Ref.
Ru/HT	393 K, 12 h, O_2 (1 bar)	126/100	94.8	97	1
SBA-NH_2-Cu^{2+} and SBA-NH_2-VO^{2+}	110 ℃, 6 h, O_2 (20 mL/min)	100/130	98.8	63.5	2
Polyaniline-VO(acac)$_2$	110 ℃, 12 h, O_2 (30mL/min)	100/80	99.2	86.8	3
Ru-6C-1N	105 ℃, 6 h, O_2 (1 bar)	126/45	94	89	4
Fe_3O_4@SiO_2-NH_2-Ru(III)	110 ℃, 4 h, O_2 (20 mL/min)	100/150	99.7	87.1	5
Fe_2O_3@HAP-Ru	90 ℃, 12 h, O_2 (20 mL/min)	100/150	100	89.1	6
V-g-C_3N_4	130 ℃, 12 h, O_2 (1 bar)	126/100	>99	82	7
Fe_3O_4/Mn_3O_4	120 ℃, 12 h, O_2 (20 mL/min)	126/160	100	82.1	8
V_2O_5/H-beta	100 ℃, 5.5 h, O_2 flow (1 bar)	100/100	84	>99	9
K-OMS-2	110 ℃, 6 h, O_2 (10 mL/min)	126/100	100	99	10
PMIN-2(V)	120 ℃, 3 h, O_2 balloon 1.0 bar	100.8/10	100	86.8	11
GO	140 ℃, 24 h, O_2 (20 mL/min)	252/20	100	90	12
α-CuV_2O_6	**130 ℃, 3 h, O_2 balloon 1.0 bar**	**126/40**	**100**	**>99**	**This work**

[a]Temperature, reaction time and pressure of O_2 for T, t and P respectively. [b]HMF conversion. [c]Selectivity of DFF.

Table S4. The catalytic performances in the synthesis of DFF from fructose over various heterogeneous catalysts.

Catalyst	T, t & P[a]	Fruc./Catalyst (mg/mg)	Y_{DFF}[b] (%) One-step	Y_{DFF}[b] (%) Two-step	Ref.
graphene oxide	140 ℃, 24 h, O_2 (20 mL/min)	360/20	53	72.5(64.5)	13
Amberlyst-15 and polyaniline-VO(acac)$_2$	110 ℃, 12 h, O_2 (20 mL/min)	145/100/80[c]	42.1	71.1	14
$Cs_3HPMo_{11}VO_{40}$	120 °C, 6 h, O_2 (0.1 MPa)	200/150	-	60(53)	15
$Cs_{0.5}H_{2.5}PMo_{12}$	160 ℃, 2 h, air	45/15	69.3(65.3)	-	16
γ-Fe_2O_3@HAP-Ru and Fe_3O_4@SiO_2-SO_3H	110 ℃, 27 h, O_2 (20 mL/min)	143/150/150[c]	-	79.1	6
g-C_3N_4(H^+) and V-g-C_3N_4	130 ℃, 8 h, O_2 (0.1 MPa)	200/100/100[c]	45	63	7
Fe_3O_4-SBA-SO_3H and K-OMS-2	110 ℃, 8 h, O_2 (10 mL/min)	180/100/100[c]	-	80	10
Ru/HT and Amberlyst-15	110 ℃, 12 h, O_2 (20 mL/min)	200/200/100[c]	-	49	17
Amberlyst 15 and SBA-15-Biimidazole-Ru	110 ℃, 14 h, O_2 (20 bar)	-	-	72.4	18
Fe/C–S	110 ℃, 5 h, O_2 (1 bar)	216/25.3	-	>99	19
P(EVPI-Br)-α-CuV_2O_6	**135 ℃, 3.5 h, O_2 (0.1 MPa)**	**180/50/90**[c]	**63.1(63)**	**76.1**	**This wok**

[a]Temperature, reaction time and pressure of O_2 for T, t and P respectively. [b]DFF yield; the value in the bracket is the yield after several recycles. [c]The weight ratio of fructose/acid catalyst/redox catalyst for the binary catalysts.

References

1 A. Takagaki, M. Takahashi, S. Nishimura, K. Ebitani, *ACS Catal*. 2011, **1**, 1562-1565.

2 X. X. Liu, J. F. Xiao, H. Ding, W. Z. Zhong, Q. Xu, S. P. Su, D. Yin, *Chem. Eng. J.* 2016, **283**, 1315-1321.

3 F. H. Xu, Z. H. Zhang, *ChemCatChem* 2015, **7**, 1470-1477.

4 Y. Q. Zhu, X. Liu, M. N. Shen, Y. G. Xia, M. Lu, *Catal. Commun*. 2015, **63**, 21-25.

5 S. G. Wang, Z. H. Zhang, B. Liu, J. L. Li, *Ind. Eng. Chem. Res.* 2014, **53,** 5820-5827.

6 Z. H. Zhang, Z. L. Yuan, D. G. Tang, Y. S. Ren, K. L. Lv, B. Liu, *ChemSusChem* 2014, **7**, 3496-3504.

7 J. Z. Chen, Y. Y. Guo, J. Y. Chen, L. Song, L. M. Chen, *ChemCatChem* 2014, **6**, 3174-3181.

8 B. Liu, Z. H. Zhang, K. L. Lv, K. J. Deng, H. M. Duan, *Appl. Catal. A* 2014, **472**, 64-71.

9 I. Sádaba, Y. Gorbanev, S. Kegnæ, S. Putluru, R. W. Berg, A. Riisager, *ChemCatChem* 2013, **5**,

284-293.

10 Z. Z. Yang, J. Deng, T. Pan, Q. X. Guo, Y. Fu, *Green Chem.* 2012, **14**, 2986-2989.

11 G. J. Chen, W. Hou, J. Li, X. C. Wang, Y. Zhou, J. Wang, *Dalton Trans.* 2016, **45**, 4504-4508.

12 C. Laugel, B. Estrine, J. L. Bras, N. Hoffmann, S. Marinkovic, J. Muzart, *ChemCatChem* 2014, **6**, 1195-1198.

13 G. Q. Lv, H. L. Wang, Y. X. Yang, T. S. Deng, C. M. Chen, Y. L. Zhu, X. L. Hou, *Green Chem*. 2016, **18**, 2302-2307.

14 F. H. Xu, Z. H. Zhang, *ChemCatChem* 2015, **7**, 1470-1477.

15 R. L. Liu, J. Z. Chen, L. M. Chen, Y. Y. Guo, J. W. Zhong, *ChemPlusChem* 2014, **79**, 1448-1454.

16 Y. Liu, L. F. Zhu, J. Q. Tang, M. Y. Liu, R. D. Cheng, C. W. Hu, *ChemSusChem* 2014, **7**, 3541-3547.

17 A. Takagaki, M. Takahashi, S. Nishimura, K. Ebitani, *ACS Catal.* 2011, **1**, 1562-1565.

18 F. Wang, L. Jiang, J. Wang, Z. H. Zhang, *Energy Fuels* 2016, **30**, 5885-5892.

19 R. Q. Fang, R. Luque, Y. W. Li, *Green Chem.* 2016, DOI: 10.1039/C6GC02018F.